Temperature and Strain-Rate Dependences of Mechanical Anisotropy of Zircaloy

K.L. Murty
North Carolina State University, Dept. of Nuclear Engineering, Box 7909, Raleigh, North Carolina 27695-7909, U.S.A.

ABSTRACT

The temperature dependence of the tensile characteristics was investigated along the axial and hoop directions of Zircaloy-4 tubing using constant strain-rate tensile tests on axial and ring tensile specimens with reduced gauge sections. Tests were performed at temperatures ranging from ambient to 773K. In addition, load relaxation tests were conducted along both axial and hoop directions to evaluate the strain-rate dependence of the strength ratios. The contractile strain-ratio, R, was evaluated from biaxial strains in uniaxial tensile tests along the axial direction while the P parameter was calculated using R and uniaxial hoop and axial stresses. Within the experimental scatter, R parameter was essentially constant. On the other hand, P parameter decreased with increase in temperature or decrease in strain-rate resulting in lower hoop strength (relative to axial) at high (>573k) temperatures and low ($<10^{-5}$ sec^{-1}) strain-rates. Those results have important implications on multiaxial deformation charateristics of Zircaloy tubing. In addition, these anisotropy parameters influence the formability of these tubing materials.

1. INTRODUCTION

The mechanical properties of hexagonal close packed (hcp) metals such as Zircaloy are sensitive to fabrication variables and the resulting crystallographic textures [1-3]. The limited number of slip systems along with the inherent anisotropy of hexagonal crystal structure renders these materials highly textured with nonrandomly oriented grains. These preferred orientations are responsible for the resulting mechanical anisotropy of Zircaloy. The characterization of the mechanical anisotropy of the cladding tubes is important in predicting the dimensional changes of the fuel cladding in service as well as in accounting for the pellet cladding mechanical interaction (PCMI). For fuel fabrication, knowledge of these parameters for Zircaloy TREX (tube reduced extrusions) and intermediate size tubing is vital for deciding on specific fabrication schedule with the final product formed uniformly without any defects or cracks. The multiaxial deformation behavior of these materials is very sensitive to the crystallographic texture and the resulting mechanical anisotropy. While the effects of fabrication parameters on mechanical anisotropy were investigated by

several authors [2, 4, 5], relatively little attention has been devoted to the effects of test variables such as the temperature and strain-rate. It is to be noted that the mechanical anisotropy parameters evaluated from multiaxial creep tests on Zircaloy cladding are quite different from those obtained from tensile tests at lower temperatures and higher strain-rates [6, 7]. Thus, while the hoop strength is higher at low temperatures and/or high strain-rates, the axial direction is stronger at high temperatures and/or low strain-rates corresponding to creep conditions. Present study has been undertaken to systematically investigate the effects of test temperature and applied strain-rate on uniaxial strengths along the hoop and axial directions of Zircaloy-4 tubing. Tensile tests were performed to evaluate the effect of test temperature while the strain-rate dependence was investigated using load relaxation tests.

2. EXPERIMENTAL

Zircaloy-4 tubing of 17.9mm outside diameter and 1.9mm thickness (intermediate size) was received in cold-worked stress-relief annealed condition. The tubing was tested in the as-received condition and exhibited crystallographic texture pole-figures with the typical basal pole peak intensities at about ±30° from radial direction while the prism pole intensity is restricted to the region ±75° from the axial direction. In addition to the basal (0002) and prism (10T0) pole-figures, pyramidal (10T2) pole-figure was also obtained to evaluate the orientation distribution function (ODF) for the material [8]. The ODF was defined in the space of Euler angles using the series method of Bunge [9] and Roe [10]. Computational details may be found in the reference [8] and Fig. 1 is a compilation of the Euler plots at constant ϕ angles with ψ versus Θ iso-intensity lines; the definition of these angles is shown in the figure also. Peak values in units of times-random intensity are given, and the intensity contours are evenly spaced in times random units. Maximum intensity was obtained to be ~8 times the random value at ϕ=0° and 60° while Adams and Murty [8] observed much higher values (~700) in cold-worked stress-relieved Zircaloy cladding. These differences are attributed to the relatively large amounts of reductions received by the cladding in the fabrication process from intermediate size to the final cladding dimensions. It is interesting to note that similar peak intensity values were noted in annealed Zircaloy cladding by Adams and Murty [8] although the peaks were noted at ϕ=30° along with more randomization process in their annealed materials.

Axial tensile tests were performed on the as-received tubing using Swazelok connectors at the tube-ends by pulling on the tubing and the connector. Stainless-steel sleeves at grip locations eliminated slippage during tensile testing. Details of the experimental procedure and measurement technique were already presented elsewhere [2, 11]. The effect of temperature on flow stress was evaluated from these tests conducted at various test temperatures under constant cross-head speed (~strain-rate). The R parameter was evaluated from diametral contraction at ~4% axial strain:

$$R = - \left(1 + \frac{\varepsilon_z}{\varepsilon_\theta}\right)^{-1} \qquad \text{eq. (1).}$$

Ring tensile specimens were machined to the design shown in Fig. 2. Two diametrically opposed reduced gauge sections were machined, and the specimens were tested in tension by circumferentially loading with platens machined to match the ID curvature of the tubing with the loading axis along the center line of the specimen (Figure 2). Strains were computed from the load-displacement curves and tests were performed at constant displacement rates at various temperatures from ambient to ~723K.

The strain-rate dependence of the mechanical anisotropy can be best inferred from load relaxation tests such as those proposed and extensively used on many different materials by Hart and Li [11-13]. Such load relaxation tests were performed at a constant temperature of 658K on both the axial and hoop tensile specimens by loading the specimens to the point of maximum load (tensile strength) at which point the crosshead was stopped and load was monitored as a function of time. The stress versus strain-rate results were evaluated from load-time data following the procedures outlined in references 11 and 13.

3. EXPERIMENTAL RESULTS

The temperature dependences of the axial and hoop tensile strengths are depicted in Figures 3a and 3 b at two different strain-rates: $1x10^{-2}$ sec^{-1} and $1x10^{-4}$ sec^{-1}. These strain-rates are the engineering values evaluated from

$$\dot{\epsilon} = \frac{\dot{X}}{\ell} \qquad \text{eq. (2).}$$

where ℓ is the appropriate gauge length, $\dot{X}$ the cross-head speed and $\dot{\epsilon}$ the strain-rate. The engineering strain-rates calculated from Eq. (2) are essentially identical to the true strain-rate values at the maximum load (i.e. ultimate tensile strength) at which the rate of change of load with time is zero. These data reveal that the temperature dependence of the relative magnitudes of the hoop and axial tensile strengths is itself a function of the applied strain-rate. This is better depicted from load relaxation data obtained at a constant temperature. Figure 4 depicts the strain-rate dependence of the axial and hoop tensile strengths at 658K, and the ratio of the hoop to axial tensile strengths is illustrated in Figure 5a as a function of the applied strain-rate. The temperature variation of this ratio is shown in Figure 5b at the two strain-rates. For a truly isotropic material, both the hoop and axial strengths would be identical at all of the test temperatures and strain-rates. The deviation from equality, and the temperature and strain-rate variations as depicted in Figures 5a and 5b are the result of the crystallographic texture and the accompanied mechanical anisotropy of Zircaloy tubing.

The R parameters, evaluated from axial tensile tests, revealed a constant value of 1.50 ± 0.45 independent of both the test temperature and the applied strain-rate. Essentially similar findings were reported earlier by Murty and Adams [7], Beauregard et al [2], and recently Baty et al [14]. Relatively large error (± 30%) in R values is indicative of the crude technique used here in determining the transverse contractile strains.

4. DISCUSSION

Before evaluating the mechanical anisotropy parameters from these data a brief discussion of the multiaxial flow analysis is presented. Hill [15] proposed a modified Von-Mises yield criterion for an anisotropic material with the applied stress axes coincident with the axes of anisotropy. In the case with no shear stresses the yield condition in cylindical coordinates is

$$F(\sigma_z-\sigma_\theta)^2 + G(\sigma_\theta-\sigma_r)^2 + H(\sigma_r-\sigma_z)^2 = 1, \qquad \text{eq. (3).}$$

where F, G and H are the coefficients of anisotropy and σ_z, σ_θ and σ_r are the principal stresses along the axial, hoop and radial directions, respectively of the tubing. The anisotropy coefficients are related to the uniaxial yield strengths along the three principal directions. Backofen [16] modified Hill's formulation by reducing the number of anisotropy coefficients from three to two, called R and P, defined as

$$R = \frac{F}{H}, \qquad P = \frac{F}{G} \qquad \text{eq. (4)}$$

Thus, Hill's equation is rewritten in terms of R and P as

$$\begin{aligned} R(\sigma_r-\sigma_\theta)^2 + RP(\sigma_\theta-\sigma_z)^2 + P(\sigma_z-\sigma_r)^2 &= P(R+1)\ Y_z^2 \\ &= R(P+1)\ Y_\theta^2 \\ &= (R+P)\ Y_r^2 \end{aligned} \qquad \text{eq. (5).}$$

Here Y_θ, Y_z and Y_r are the yield stresses along the hoop, axial and radial directions of the tubing respectively. Following the convention adopted by Woods [17] and Duncombe [18], a generalized stress σ_g is defined as the uniaxial yield stress along the axial direction so that the yield criterion reads as follows:

$$\sigma_g^2 = \frac{R(\sigma_r-\sigma_\theta)^2 + RP(\sigma_\theta-\sigma_z)^2 + P(\sigma_z-\sigma_r)^2}{P(R+1)} \qquad \text{eq. (6).}$$

Using the Prandtl-Reuss energy balance and equation (6), the strain increments or rates along the radial, hoop and axial directions are related to the respective stresses according to the following:

$$\begin{pmatrix} \dot{\varepsilon}_r \\ \dot{\varepsilon}_\theta \\ \dot{\varepsilon}_z \end{pmatrix} = \frac{\dot{\varepsilon}_g}{P(R+1)\sigma_g} \begin{bmatrix} R+P & -R & -P \\ -R & R(P+1) & -RP \\ -P & -RP & P(R+1) \end{bmatrix} \begin{pmatrix} \sigma_r \\ \sigma_\theta \\ \sigma_z \end{pmatrix} \qquad \text{eq. (7)}$$

Here $\dot{\varepsilon}_g$ is equivalent to the uniaxial strain rate determined in a cylindrical specimen loaded axially to a stress equal in magnitude to σ_g. Thus, a knowledge of the anisotropy parameters (R, P) in conjunction with the above two equations 6 and 7 enables a complete characterization of the multiaxial deformation behavior of an anisotropic material. For uniaxial loading along the axial and hoop directions, we find that

$$\left(\frac{\dot{\varepsilon}_\theta}{\dot{\varepsilon}_r}\right)_{\varepsilon_z} = R \,, \qquad \sigma_\theta = \sigma_r = 0$$

$$\left(\frac{\dot{\varepsilon}_z}{\dot{\varepsilon}_r}\right)_{\varepsilon_\theta} = P \,, \qquad \sigma_z = \sigma_r = 0 \qquad \text{eq. (8).}$$

These equations imply that the two coefficients of anisotropy, P and R, are given by the transverse contractile strain (rate) ratios in the uniaxial hoop and axial tests, respectively. For the special case of equibiaxial loading ($\sigma_\theta = \sigma_z$), the hoop to axial strain-rate ratio is given by

$$\frac{\dot{\varepsilon}_\theta}{\dot{\varepsilon}_z} = \frac{R}{P} \qquad \text{eq. (9).}$$

For an isotropic material with R = P = 1, therefore, the strain-rate ratio should be unity.

The ratio of the anisotropy parameters can be evaluated from a knowledge of the uniaxial tensile strengths along the axial and hoop directions at various temperatures and strain-rates. From the above formulations we note that the ratio of the hoop to axial strengths is related to the anisotropy parameters:

$$\left(\frac{S_\theta}{S_z}\right)^2 = \frac{P(R+1)}{R(P+1)} \,, \qquad \text{eq. (10).}$$

where S_θ and S_z are the tensile strengths along the hoop and axial directions, respectively, of the tubing. Using the R value of 1.5, the parameter P can be evaluated from the uniaxial tensile strengths from eq. (11),

$$P = \frac{(S_\theta/S_z)^2}{1.67-(S_\theta/S_z)^2} \qquad \text{eq. (11).}$$

The temperature and strain-rate dependences of the P-parameter are evaluated using the data in figure 5 and the above eq. (11) and are depicted in figures 6a and 6b. Results obtained from load relaxation data are compared in Figure 6b with the tensile test results at constant applied strain-rates. Whereas R parameter is essentially independent of both the test temperature and applied strain-rate, P parameter decreased from ~1.6 at ambient temperature and relatively high strain-rates to ~0.25 at high temperatures and relatively low strain-rates. As noted in figures 6a and 6b, the P parameter decreased as temperature increases and/or strain-rate decreases. It is interesting to note that the R parameter is also relatively insensitive to the annealing temperature following a given amount of cold-work while P parameter increases with the annealing temperature [2, 19].

5. CONCLUSIONS

Experimental results revealed that the R parameter is relatively insensitive to the test variables within the range adopted here. In contrast, the P parameter was

noted to be sensitive to both the test temperature and the applied strain-rate. The tensile strength along the hoop direction is slightly greater than that along the axial direction, as is generally believed, at temperatures below about 323K and at relatively high strain-rates. However, at higher temperatures and lower strain rates, the hoop direction is seen to be weaker than the axial. The ratio of hoop to axial tensile strengths is found to be a function of the test temperature as well as the applied strain-rate. This is important to note since it is generally, but mistakenly, assumed that the hoop direction is always stronger than the axial. The present finding is in agreement with some recent creep results on Zircaloy cladding [6,7,14,19], which revealed that at temperatures greater than about 573K the hoop creep-rate is ~6-10 times that of the axial creep-rate under equibiaxial loading implying (see eq.9) that P parameter is about 6-10 times smaller than R. This rapid decrease in the P value at elevated temperatures resulted in relatively weaker hoop direction. Equal strengths along the hoop and axial directions are realized when R=P. Present results demonstrate the significance of the effect of test variables on the mechanical anisotropy parameters. More detailed experimental results are needed to quantify the functional dependence of the anisotropy parameters on the test temperature and the applied strain-rate.

ACKNOWLEDGEMENTS

I wish to acknowledge the financial support by the National Science Foundation under grant DMR-8313157. Various discussions with my previous collaborators, Professor B. L. Adams of Brigham Young University, Drs. G. P. Sabol and S. G. McDonald of Westinghouse Research and Development Center contributed to many of the ideas presented here. Thanks are due to Judy Mudd for preparing the manuscript.

REFERENCES

/ 1/ Kallstrom, K., "Texture and Anisotropy of Zirconium in Relation to Plastic Deformation," Can. Metallurg. Quart. 11, 185-198 (1972)

/ 2/ Beauregard, R. J., Clevinger, G. S., Murty, K. L., "Effect of Annealing Temperature on the Mechanical Properties of Zircaloy-4 Cladding," Proceedings, Fourth International Conference on Structural Mechanics in Reactor Technology, San Francisco, August 1977, Paper C3/5.

/ 3/ Kallstrom, K., Andersson, T., Hofvenstam, A., "Creep Strength of Zircaloy Tubing at 400C as Dependent on Metallurgical Structure and Texture," in 'Zirconium in Nuclear Applications,' ASTM STP551 160-168 (1974).

/ 4/ Frenkel, J. M., Weisz, M., "The Influence of Various Metallurgical Parameters and Neutron Flux On Creep of Zircaloy-4 Cladding Tubes," International Conference on Nuclear Fuel Performance, London, Oct. 1973.

/ 5/ Stehle, H., Steinberg, E., Tenckhoff, E., "Mechanical Properties, Anisotropy and Microstructure of Zircaloy Canning Tubes," in 'Zirconium in the Nuclear Industry,' ASTM STP 633, 488-507 (1977).

/ 6/ Murty, K. L., "Biaxial Creep of Zircaloy Cladding," in Proceedings, International Conference on Deformation, Ranchi, March 17, 1983.

/ 7/ Murty, K. L., Adams, B. L., "Multiaxial Creep of Textured Zircaloy-4," in 'Mechanical Testing for Deformation Model Development,' ASTM STP 765, 382-396 (1982).

/ 8/ Adams, B. L., Murty, K. L., "Biaxial Creep of Textured Zircaloy: Part II. Crystal-Mean Plastic Modelling," Mater. Sci. Eng., in print.

/ 9/ Bunge, H. J., Z. Metallk. 56, 872 (1965).

/10/ Roe, R.J., J. Appl. Phys. 36, 2024 (1965).

/11/ Murty, K. L., McDonald, S. G., "Tensile, Creep and Load Relaxation Characteristics of Zircaloy Cladding at 300C," Proceedings, Sixth International Conference on Structural Mechanics in Reactor Technology, Berlin, paper C3/6 (1979).

/12/ Hart, E. W., "Constitutive Relations for the Non-elastic Deformation of Metals," J. Eng. Mat. Tech., 98H, 193 (1976)

/13/ Huang, F. H., Sabol, G. P., McDonald, S. G., Li, Che-Yu., "Load Relaxation Studies of Zircaloy-4," J. Nucl. Mater., 79, 214 (1979).

/14/ Baty, D. L., Pavinich, W. A., Dietrich, M. R., Clevinger, G. S., Papazoglou, T. P., in 'Zirconium in the Nuclear Industry,' ASTM STP 824, 306 (1984).

/15/ Hill, R., Proc. Roy. Soc. (Lond.), 193A, 281 (1948)

/16/ Backofen, W. A., "Deformation Processing," Addison-Wesley (New York) 1972.

/17/ Woods, C. R., "Properties of Zircaloy-4 Cladding," WAPD-TM - 585, Westinghouse Electric Co., Dec. (1966).

/18/ Duncombe, E., Friedrich, E. M., Guilinger, W. H., Nucl. Tech., 12, 194 (1971).

/19/ Murty, K. L., Adams, B. L., "Biaxial Creep of Textured Zircaloy: Part I. Experimental and Phenomenological Descriptions," Mater. Sci. Eng., in print.

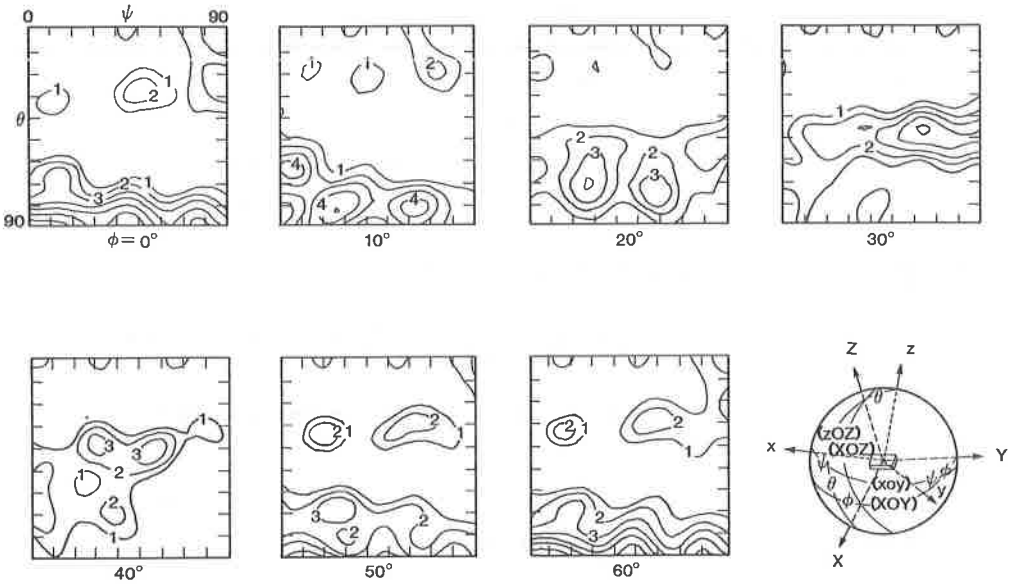

Fig. 1. Euler plots representing the orientation distribution function for cold-worked stress-relieved Zircaloy tubing are shown at constant intervals of 10° as iso-intensity levels. The chosen Euler coordinates are shown in the bottom right hand corner. Times random-intensity values are indicated for certain contours, and others are evenly spaced.

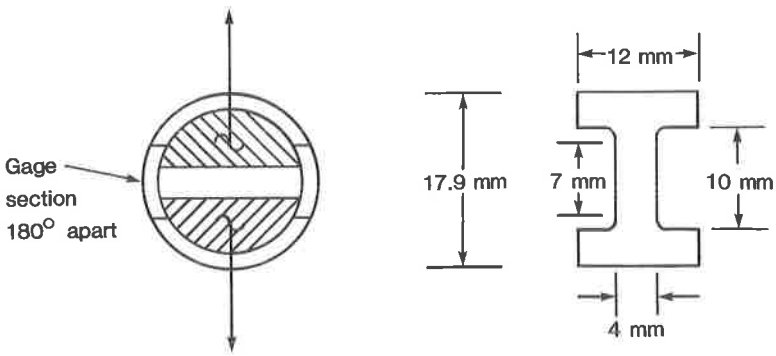

Fig. 2. Design Of Ring Tensile Specimens.

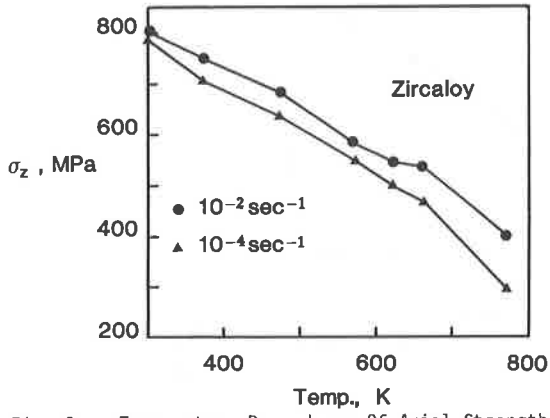

Fig. 3a. Temperature Dependence Of Axial Strength.

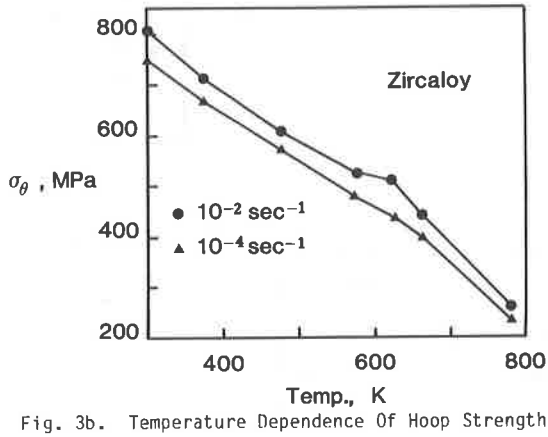

Fig. 3b. Temperature Dependence Of Hoop Strength.

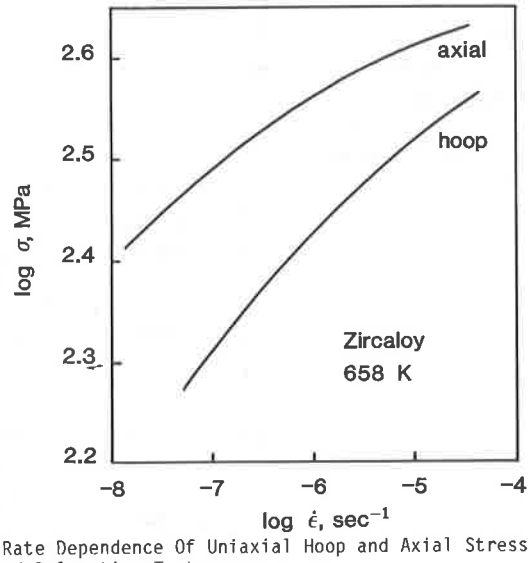

Fig. 4. Strain-Rate Dependence Of Uniaxial Hoop and Axial Stress at 658K Obtained From Load Relaxation Tests.

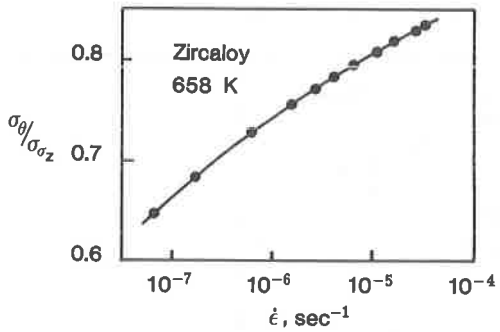

Fig. 5a. Ratio Of Hoop To Axial Stress Versus Strain-Rate.

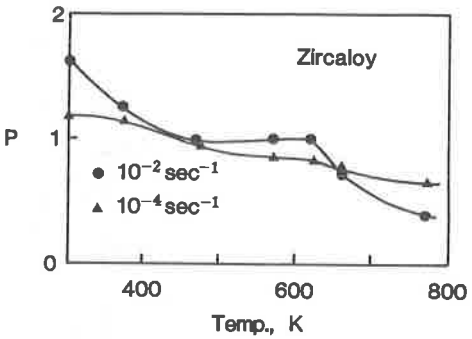

Fig. 6a. Temperature Dependence Of P-Parameter.

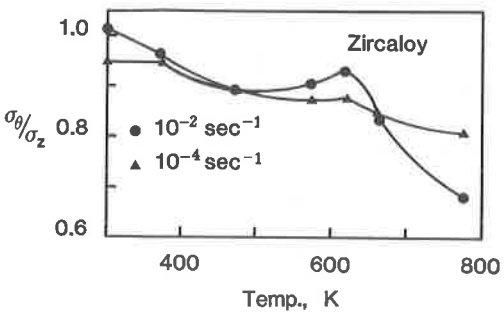

Fig. 5b. Temperature Variation Of Hoop To Axial Stress Ratio At Two Different Strain-Rates.

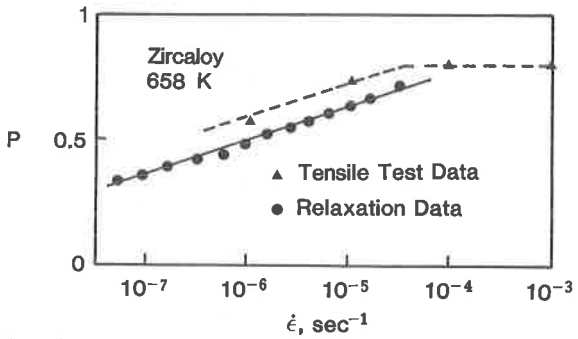

Fig. 6b. Strain-Rate Dependence Of P-Parameter. Relaxation data are compared with tensile test results.